



# Determination of phase change temperature of materials from adiabatic scanning calorimetry data

Igor Medved<sup>1,3</sup> · Milan Jurči<sup>1</sup> · Anton Trník<sup>2,3</sup>

Received: 18 August 2021 / Accepted: 20 March 2022 / Published online: 28 April 2022  
© Akadémiai Kiadó, Budapest, Hungary 2022

## Abstract

Melting and other first-order phase changes usually occur in phase change materials (PCMs) within a noticeable temperature range rather than at a unique phase change temperature ( $T_{pc}$ ). Then the enthalpy and heat capacity have rather wide jumps and peaks, respectively, spread over such ranges of temperatures. Surprisingly, wide jumps and peaks are observed even in plain and simple cases when PCMs are pure substances with negligible hysteresis and/or supercooling and the measurements are quasi-equilibrium using very slow heating/cooling rates, as in adiabatic scanning calorimetry (ASC). We show that in such cases a unique  $T_{pc}$  can be identified and calculated from the measured heat capacity peaks. It suffices to take into account that PCM samples do not have an ideal microstructure but are rather composed of many micro- to nano-sized domains. The heat capacity peak is then an average of individual peaks that (a) come from all domains and (b) have different shifts from  $T_{pc}$  for different domain sizes. Interpreting a heat capacity peak measured by ASC in this way, we present a procedure from which  $T_{pc}$  can be evaluated. We apply the procedure to three examples of materials using available ASC data and point out the importance of the size distribution of domains.

**Keywords** Heat capacity peak · First-order phase change · Domain size distribution · Averaging

## Introduction

Phase change materials (PCMs) have been widely used for thermal energy storage in various applications, such as energy conservation in buildings with thermal comfort [1], smoothing of temperature fluctuations [2], cold storage [3, 4] and passive cooling in building envelopes [5], solar energy storing [6] and solar thermal power plants [7, 8],

thermal management systems [9, 10], or textiles and clothing systems [11]. Such applications make use of the ability of materials to store or release a large amount of energy during a first-order phase change. In PCMs the predominant part of this energy is due to the latent heat, while the sensible heat is much smaller (by an order or two in the magnitude). Thus, the primary characteristics needed for a proper design and correct performance of PCM systems include the specific latent heat,  $\ell$ , and the temperature of a phase change,  $T_{pc}$ , at which  $\ell$  is released (or absorbed).

From the viewpoint of thermodynamics, a first-order phase change is associated with a jump in the enthalpy. The jump is considered to be infinitely sharp, so that (a) it occurs at a unique temperature ( $T_{pc}$ ) and (b) its size ( $\ell$ ) is well defined. In real PCMs the jumps are not infinitely sharp, however. Instead, they are spread out over a range of temperatures to be called ‘a phase change region’ in the following. Then the determination of  $\ell$  and  $T_{pc}$  (and other thermal properties of PCMs) is a rather challenging task, and various approaches and methods have been proposed to deal with this problem [12]. In this paper we wish to provide an approach from which  $T_{pc}$  of real PCMs can be determined

✉ Igor Medved<sup>1</sup>  
igor.medved@stuba.sk

Milan Jurči  
milan.jurci@stuba.sk

Anton Trník  
atrnik@ukf.sk

<sup>1</sup> Department of Materials Engineering and Physics, Faculty of Civil Engineering, Slovak University of Technology, 81005 Bratislava, Slovakia

<sup>2</sup> Department of Physics, Constantine the Philosopher University, 94974 Nitra, Slovakia

<sup>3</sup> Department of Materials Engineering and Chemistry, Faculty of Civil Engineering, Czech Technical University, 16629 Prague, Czech Republic

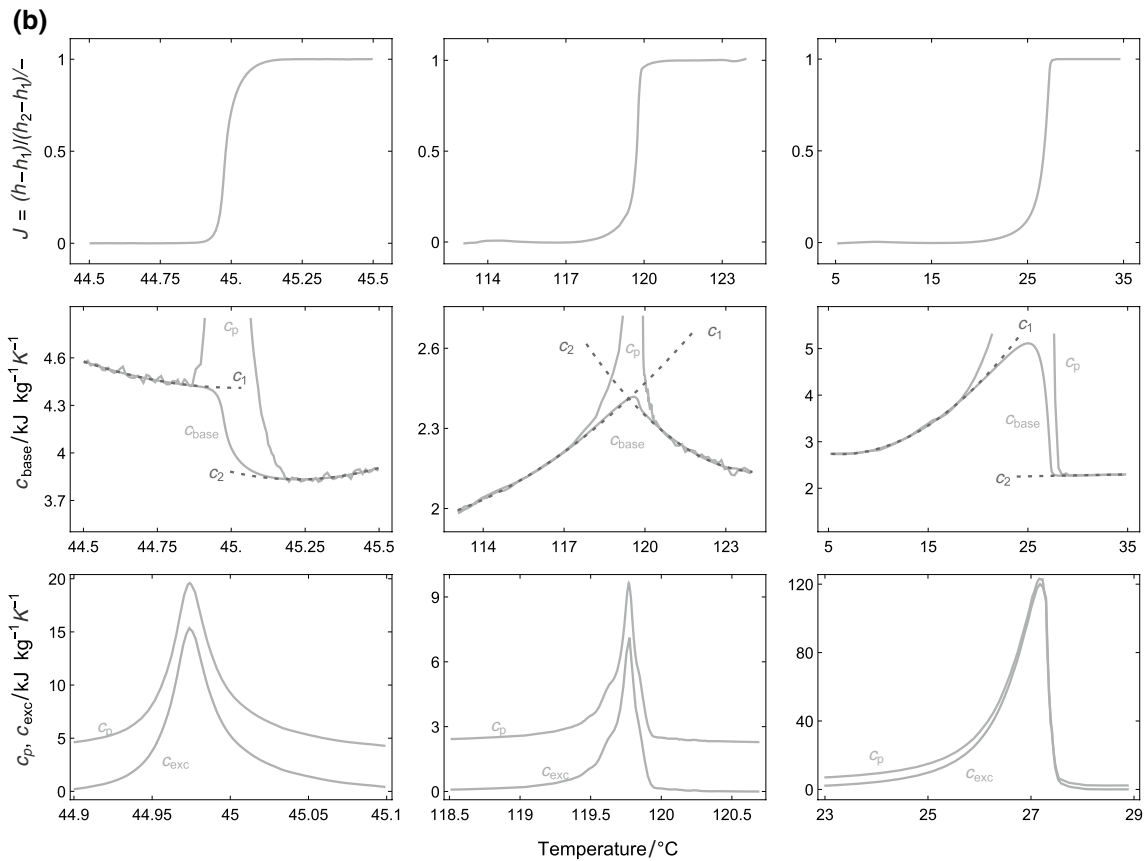
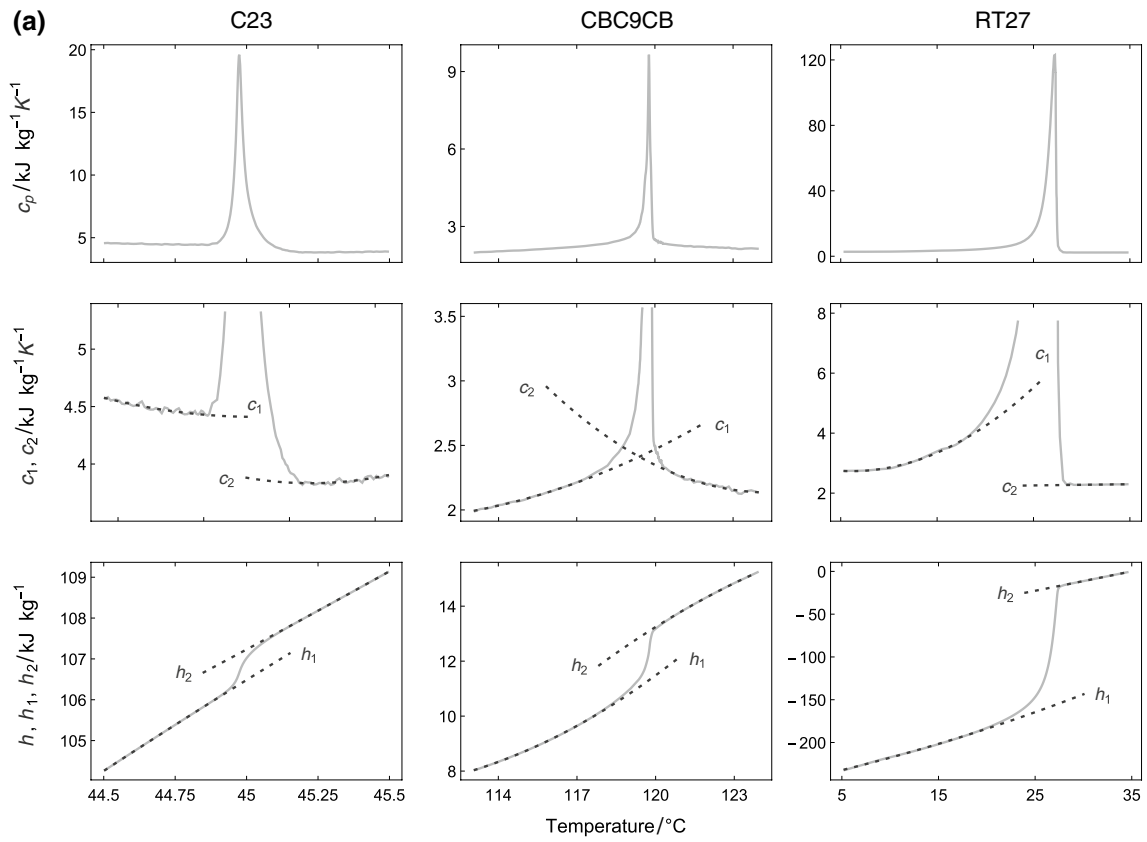


**Fig. 1 a** The temperature dependences of the heat capacity and enthalpy (the full lines) for three materials and their phase changes obtained from ASC measurements (adapted from [14–16]). The heat capacities and enthalpies of the two phases (the dashed lines) are obtained as approximation by quadratic polynomials [13]. **b** The separation of the sensible and latent heats ( $c_{\text{base}}$  and  $c_{\text{exc}}$ , respectively)

as a theoretical value at which an infinitely sharp enthalpy jump would occur.

There may be various reasons why phase change regions are present. It could be due to the properties of a given PCM: it need not be a pure substance, it could have an advanced microstructure, or its behavior near the considered phase change can be nontrivial (it may exhibit true thermal hysteresis, supercooling, etc.). Or, the applied experimental techniques could operate under conditions that make the interpretation of the measured data difficult. For example, fast heating/cooling rates may be used (then the material is not close to its equilibrium and kinetic effects could be strong) or samples may have large sizes (various parts of samples would be in different thermal states).

Therefore, to avoid these complications, in [13] we considered first-order phase changes in PCMs for simple but nontrivial cases and proposed their theoretical description. Namely, we assumed that phase changes in PCMs were free from additional effects (such as thermal hysteresis or supercooling) and that kinetic effects were negligible (i.e., during the measurement the material was close to its equilibrium). We applied our results to the following three examples of materials and their phase changes:

- a pure linear alkane tricosane  $\text{C}_{23}\text{H}_{48}$  (denoted here as C23) in which a change between two rotator phases occurs near  $45^\circ\text{C}$ ;
- a pure liquid crystal dimer  $\alpha$ ,  $\omega$ -bis(4,4'-cyanobiphenyl) nonane (denoted here as CBC9CB) in which isotropic–nematic transition takes place near  $120^\circ\text{C}$ ; and
- a paraffin-based PCM called Rubitherm RT27 in which a melting between a solid and liquid phases occurs near  $27^\circ\text{C}$ .

While RT27 has a rather high latent heat and is used as a PCM for practical purposes, this is not so for the other two materials. They are considered here to demonstrate the diversity of the presented results. The enthalpies and heat capacities near phase changes (a)–(c) had been measured by adiabatic scanning calorimetry [14–16] (see Fig. 1), both with a relative standard uncertainty of 2% [17]. In this experimental technique extremely low heating/cooling scanning rates are used, so that the studied samples remain very close to their thermodynamic equilibrium states. In the three cases (a)–(c) the applied scanning rates did not exceed  $0.01 \text{ K min}^{-1}$  (the relative standard uncertainty being

$10^{-4}$  on the rate and  $10 \mu\text{K}$  on the temperature measurement [17]). Moreover, thermal hysteresis and supercooling were practically absent. Even then phase change regions were still evident: the widths of the corresponding enthalpy jumps and heat capacity peaks were  $0.06 \text{ K}$  for C23,  $0.24 \text{ K}$  for CBC9CB, and  $1.56 \text{ K}$  for RT27 (see Fig. 1a). Therefore, these phase change regions must be of purely equilibrium nature, and in [13] we were able to explain them as a result of finite-size (i.e., surface) effects [18].

Our explanation of the phase change regions by surface effects provided in [13] is somewhat indirect, however. The reason is that for common sample sizes these effects would not yield any noticeable phase change regions. Instead, enthalpy jumps and heat capacity peaks would be extremely narrow and sharp. In other words, phase change regions of proper widths would occur only for unrealistically small samples (of few nanometers) [13]. Nevertheless, these conclusions are true only when samples are assumed to have perfect microstructure. The microstructure of a real material, even when it is in a single phase, is far from being perfect, however. That is why in [13] we considered a material to be a huge conglomerate of various parts, segments, or domains each of which has a perfect, uniform microstructure (see Fig. 2) and whose exact meaning depends on a given PCM. Then the jumps and peaks are not results of surface effects in the material as a whole but in the individual domains. Thus, the sample size, or the sizes of grains in powder (or similar) materials, are not essential to the determination of quantities like the phase change temperature  $T_{\text{pc}}$ . Instead, the key feature are the sizes of domains and their distribution, which are true material properties.

Applying this approach, in [13] we were able to fit experimental jumps and peaks with our theoretical results with very good accuracy. It was also possible to separate sensible and latent heats (see Fig. 1b) and to determine the phase change temperature  $T_{\text{pc}}$  (as the temperature where the enthalpy has a discontinuity). Our approach was based on general statistical mechanical results on first-order phase transitions [19] in which it is not needed to specify the details on the phases that change in a material during a transition. It suffices to characterize the phases via their macroscopic properties: for PCMs these are the enthalpies and heat capacities of their phases. Note that all domains are in the same phase at a given temperature,  $T$ , far away from  $T_{\text{pc}}$ . However, due to surface effects [19], at  $T$  near  $T_{\text{pc}}$  some domains may be in one phase, while the remaining domains may simultaneously be in the other phase.

This approach—when macroscopic properties of a material are obtained as a sum of the corresponding microscopic properties of its many constituents—could be applied in a somewhat broader context. For instance, to crystals that contain domains where not only broad peaks but also ‘saw-like’

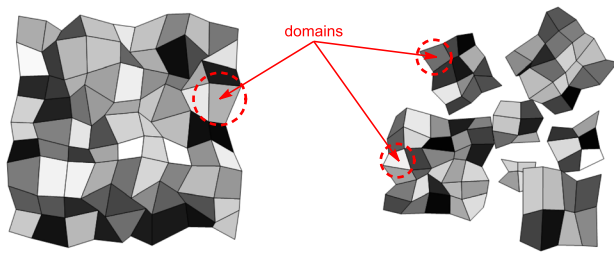


**Fig. 2** A schematic picture of domains, shown as small tetragons, in a material (left) and a granular/powder material composed of grains (right). In reality, the shapes and orientations of domains and grains are more complex. Shading is used here just to distinguish the domains. Domains may be equal to grains or could be just parts of grains. It is the sizes of these domains, and not of the sample or grains, that we use to determine a phase change temperature  $T_{pc}$

peaks are observed near polymorphic first-order phase transitions [20–25]. Or to electrode surfaces made of many crystalline domains and the corresponding sharp spikes measured in the current density during underpotential deposition of metals on electrode surfaces [26–30]. In the context of PCMs we may have in mind an example of powder materials made of many crystalline domains. Nevertheless, the approach seems to be rather robust and might be used for other types of PCMs, even when its applicability is not obvious but could bring an insight and plausible results not yet available by other approaches.

The values of  $T_{pc}$  obtained in [13] for the three materials (a)–(c) were not convincing, however, because they were too distant from the maximum of the heat capacity peak in comparison with the peak's width. Indeed, this distance relative to the width was 2.1 for C23, 3.8 for CBC9CB, and 4.2 for RT27 (see Table 1). Hence,  $T_{pc}$  would lie rather beyond the corresponding phase change regions. In this paper we wish to improve these results and provide a refined technique to determine a value of  $T_{pc}$ . It will turn out that the domain size distribution is essential for this task, which will be demonstrated by considering two simplest choices of the distribution. First, in **Theoretical background** section, we give a concise summary of results from [13] and identify the oversimplification that caused  $T_{pc}$  to be so much shifted beyond the phase change regions in [13]. Then, in **Results and discussion** section, we present an improved procedure from which  $T_{pc}$  can be determined, discuss the role of the domain size distributions, and apply the procedure to calculate  $T_{pc}$  for the three considered materials. A final section contains concluding remarks.

## Theoretical background

We consider a material that exhibits a first-order change between two phases at a certain temperature  $T_{pc}$  (the phase change temperature). Hence, at  $T_{pc}$  the enthalpy,  $h$ , has a jump of size  $\Delta h = \ell$  (the specific latent heat). The material is assumed to be composed of a large number of homogeneous parts or segments to be called domains,  $D$ . To describe macroscopic properties of such a multi-component PCM in a simple way, its partition function is supposed to be the product of the domain partition functions; i.e., the interactions between the domains are neglected. The influence of nearby surroundings on the domains is taken into account as surface effects. Then the specific heat capacity,  $c_p$ , can be expressed as a weighted average of heat capacities,  $c_D$ , due to the individual domains [13],

$$c_p = \sum_D w_D c_D. \quad (1)$$

The domain masses are equal to their mass fractions,  $w_D = m_D/m$ , where  $m = \sum_D m_D$  is the total mass of domains (equal to the mass of the PCM).

The domain heat capacities  $c_D$  can be determined from an equilibrium statistical mechanical theory of first-order phase transitions [19]. It implies that the dependence of  $c_D$  on different domains is very precisely given only via the domain diameter,  $d_D$ , and domain surface effects. The latter is expressed via a domain surface free energy difference,  $\sigma_D$ . Thus,  $c_D$  is a function  $c_D(d_D, \sigma_D)$  of these two parameters, and we may rewrite Eq. (1) in a more convenient form when we arrange the domains according to their values of  $d_D$  and  $\sigma_D$ . Namely, let  $d_1, \dots, d_n$  be all different values of domain diameters (in the ascending order). Given the domains of the same diameter  $d_i$ , let  $N_i$  be their number and let  $\sigma_{i,1}, \dots, \sigma_{i,M_i}$  be all different values of their  $\sigma_D$ . If  $N_{ij}$  is the number of domains of diameter  $d_i$  with the value of  $\sigma_D$  equal to  $\sigma_{ij}$ , then the average over domains in Eq. (1) may be written as a double average over  $d_i$  and  $\sigma_{ij}$  [13],

$$c_p = \sum_{i=1}^n N_i w_i \sum_{j=1}^{M_i} v_{ij} c_{ij}. \quad (2)$$

Here the fractions  $v_{ij} = N_{ij}/N_i$ , the masses  $w_i = d_i^3/\Omega$  with  $\Omega = \sum_{i=1}^n N_i d_i^3$ , and the domain heat capacities  $c_{ij}$  are equal to  $c_D(d_D, \sigma_D)$  with  $d_D = d_i$  and  $\sigma_D = \sigma_{ij}$ . Since  $\sum_{j=1}^{M_i} N_{ij} = N_i$ , the fractions  $v_{ij}$  are normalized to one; i.e.,  $\sum_{j=1}^{M_i} v_{ij} = 1$ .

An explicit formula

$$c_{ij} = c_{ij}^J + c_{ij}^P, \quad c_{ij}^J \approx c_1 + (c_2 - c_1)J_{ij}, \quad c_{ij}^P \approx c_0 w_i P_{ij} \quad (3)$$

can be actually obtained from an equilibrium microscopic theory [19] whenever the domain shapes are not too oblong and the surface effects are not strong. Hence,  $c_{ij}$  is a sum of

two parts. One part,  $c_{ij}^J$ , exhibits a jump that interpolates between the specific heat capacities,  $c_1$  and  $c_2$ , of the two phases involved in the phase change. The other part,  $c_{ij}^P$ , exhibits a sharp peak of area equal to the specific latent heat,  $\ell$ , and of height  $c_0 w_i$  that is larger than  $c_1$  or  $c_2$  by one or two orders of magnitude. The dimensionless functions  $0 < J_{ij} < 1$  and  $0 < P_{ij} \leq 1$  that describe this jump and peak, respectively, are

$$J_{ij} = \frac{1 + \tanh[x_i(\sigma_{ij})]}{2}, \quad P_{ij} = \cosh^{-2}[x_i(\sigma_{ij})], \quad (4)$$

with

$$x_i(\sigma) = 2w_i \frac{T - T_i(\sigma)}{\Delta T}, \quad T_i(\sigma) = \left(1 + \frac{s\sigma}{v\ell\rho d_i}\right) T_{pc}, \quad \Delta T = \frac{4k_B T_{pc}^2}{v\Omega\rho\ell}, \quad (5)$$

and  $c_0 = \ell/\Delta T$ . Here  $\rho$  is the PCM density and  $k_B$  is the Boltzmann constant. The geometric factors  $s$  and  $v$  are chosen so that the domain's surface and volume are equal to  $sd_i^2$  and  $vd_i^3$ , respectively (for example,  $s = \pi$  and  $v = \pi/6$  if domains are spherical). Note that  $T_i(\sigma_{ij})$  has the meaning of the temperature at which the domain peak is maximal (i.e., at which  $P_{ij}$  is equal to 1).

### Can the heat capacity in a single domain fit experimental data?

A single domain of diameter  $d$  cannot yield a proper heat capacity peak. In fact, if a single  $c_{ij}$  should describe the peak, then  $c_0$ ,  $\ell$ , and  $\Delta T$  would be the peak's height, area, and width, respectively. Taking their typical values from experiment, the last relation in Eq. (5) would yield the diameter  $d = (4k_B T_{pc}^2/v\rho c_0 \Delta T^2)^{1/3}$  of order 1 nm to 10 nm. Only such tiny domains would give a heat capacity peak of correct experimental proportions, while a peak from a micro domain would be several orders of magnitude taller and narrower [13].

### Separation of sensible and latent heats

Using Eqs. (2) and (3), the heat capacity of the whole PCM may be split into two parts [13],

$$c_p = c_{base} + c_{exc}. \quad (6)$$

The baseline heat capacity  $c_{base}$  has a jump of size  $\ell$  interpolating between  $c_1$  and  $c_2$ , while the excess heat capacity  $c_{exc}$  has a peak whose area is  $\ell$  and its height is much larger than  $c_1$  or  $c_2$ ,

$$c_{base} = c_1 + (c_2 - c_1)J, \quad c_{exc} = c_0P. \quad (7)$$

The jump and peak functions  $J$  and  $P$  are double averages of the domain jumps  $J_{ij}$  and peaks  $P_{ij}$  [13]: Eqs. (2) and (3) yield  $J = \sum_{i=1}^n N_i w_i \sum_{j=1}^{M_i} v_{ij} J_{ij}$  and

$$P = \sum_{i=1}^n N_i w_i^2 P_i, \quad P_i = \sum_{j=1}^{M_i} v_{ij} P_{ij}. \quad (8)$$

Note that

$$J(T) = \frac{1}{\ell} \int_{-\infty}^T c_{exc}(T) dT, \quad (9)$$

because  $\int_{-\infty}^T P_{ij} dT = (\Delta T/w_{iexti}) J_{ij}$  by Eq. (4).

Experimentally, the separation of the baseline and excess heat capacities  $c_{base}$  and  $c_{exc}$  is rather straightforward. It is based on the fact that the enthalpy  $h$  interpolates between the enthalpies  $h_1$  and  $h_2$  of the two phases involved in the phase change in the same way as  $c_{base}$ , so that the jump in  $h$  is described again by the function  $J$  [13]. Therefore, the baseline heat capacity can be determined from an experimental plot of the specific enthalpy  $h$  as

$$c_{base} = c_1 + (c_2 - c_1) \frac{h - h_1}{h_2 - h_1}. \quad (10)$$

Using this result and an experimental plot of the specific heat capacity  $c_p$ , the excess heat capacity is obtained as the difference  $c_{exc} = c_p - c_{base}$  (see Fig. 1).

### The significance of averaging

As already argued, the heat capacity peak  $c_{ij}$  from a single domain is inappropriate to fit experimental data, because the peak is too tall and narrow (unless the domain is very small). The effect of both averages in Eq. (8)—over the domain diameters and surface effects—is that the resulting, averaged peak can have a height and width of magnitudes that are measured in experiments. In fact, the domain peaks are of various heights  $c_0 w_i$  and widths  $\Delta T/w_i$  and located at different temperatures  $T_i$ , depending on the domain's size  $d_i$  and surface effects  $\sigma_{ij}$ . Hence, for sufficiently broad distributions of values of  $d_i$  and  $\sigma_{ij}$ , the averages of the tall and narrow domain peaks will be much wider and smaller, as in experiments. On the other hand, the peaks' areas are independent of  $d_i$  and  $\sigma_{ij}$  and remain unchanged after averaging.

### Surface effects

Even though the values  $\sigma_{ij}$  and fractions  $v_{ij}$  are not available from experiments, the average  $P_i = \sum_{j=1}^{M_i} v_{ij} P_{ij}$  of the domain peaks  $P_{ij}$  over surface effects can be plausibly estimated. Namely, it could be well assumed that the surface effects between different domains are irregular, so that the values  $\sigma_{ij}$  should be random. For a given domain diameter  $d_i$ , let the



surface free energy differences  $\sigma_{i,1}, \dots, \sigma_{i,M_{exti}}$  have a mean value  $\bar{\sigma}_i$  and a fluctuation (standard deviation)  $\Delta\sigma_{i,exti}$ . Since  $\sigma_{ij}$  are related to the domain surfaces, the fluctuation should be inversely proportional to the domain diameter (i.e., to the square root of the surface size), yielding  $\Delta\sigma_i = b_0/d_i$  with a constant  $b_0 > 0$  [13].

Since the number  $N_i$  is to be large (given that the number of domains in a PCM sample is huge), an appropriate approximation for the fractions  $v_{ij}$  is the Gaussian probability distribution with mean  $\bar{\sigma}_i$  and standard deviation  $\Delta\sigma_i$ . Then the summation in  $P_i$  can be well estimated by integration over  $\sigma_{ij}$ , yielding [13]

$$P_i \approx \frac{\eta}{d_i} e^{-y_i^2}, \quad \eta = \sqrt{\frac{8}{\pi}} \frac{k_B T_{pc}}{s b_0}, \quad (11)$$

$$y_i = \frac{\sqrt{\pi} \eta}{2d_i} x_i(\bar{\sigma}_i),$$

providing that  $(\eta/d_i)^2 \ll 1$ . The latter condition ensures that the distribution of values  $\sigma_{ij}$  is broad and the averaged peak  $P_i$  is much smaller and wider than the individual domain peaks  $P_{ij}$ .

### Excess heat capacity

Contrary to the distribution of values  $\sigma_{ij}$ , the distribution of domain diameters  $d_i$  for a given PCM may be obtained from experiment. Since it might change considerably from case to case, it is appropriate to leave the averaging over diameters unevaluated and do so only when the domain size distribution is known (measured). Hence, combining Eqs. (7), (8), and (11), the excess heat capacity is given as

$$c_{exc} = c_0 \sum_{i=1}^n N_i w_i^2 P_i \approx c_0 \frac{\eta}{\Omega^2} \sum_{i=1}^n N_i d_i^5 e^{-y_i^2}. \quad (12)$$

Thus, the peak exhibited by  $c_{exc}$  is a sum of symmetric, Gaussian peaks  $\exp(-y_i^2)$  whose maxima are at  $T_i(\bar{\sigma}_i)$ . These temperatures vary with the domain diameter and surface effects (represented by  $\bar{\sigma}_i$ ), and the shifts between the temperatures are unequal. The sum  $c_{exc}$  of so unevenly distributed symmetric peaks yields a peak that is asymmetric in general, as those in experiments. Moreover, the resulting peak in  $c_{exc}$  may be well expected to be much broader and smaller (even by several orders of magnitude) than any of the peaks in the sum.

As soon as a theoretical plot of the excess heat capacity vs. temperature is obtained from Eq. (12), the addition of the baseline part  $c_{base}$  from Eq. (10) gives a theoretical plot of the total heat capacity  $c_p$ .

### Oversimplification of surface effects

In [13] we applied Eq. (12) to fit heat capacity peaks obtained from experiments for the three considered materials (C23, CBC9CB, and RT27) with great accuracy. Nevertheless, the determined values of  $T_{pc}$  for the three materials do not seem satisfactory, because they all lie rather outside the corresponding phase change regions (as was already pointed out in the Introduction). The reason is that in [13] we crudely assumed all  $\bar{\sigma}_i$  to be the same for all domain diameters,  $\bar{\sigma}_i = \text{const} = \bar{\sigma}_0$ . Then the domain peaks  $\exp(-y_i \text{exti}^2)$ , their maxima being at the temperatures  $T_i(\bar{\sigma}_0)$ , were all shifted either above or below  $T_{pc}$ , depending on the sign of  $\bar{\sigma}_0$ . Thus, the resulting peak in  $c_{exc}$  had its maximum shifted too far from  $T_{pc}$ . In this study the oversimplification  $\bar{\sigma}_i = \text{const}$  is eliminated and we let  $\bar{\sigma}_i$  be varying with domain diameters.

### Results and discussion

Introducing the dimensionless quantities

$$\delta_i = \frac{d_{exti}}{d_n}, \quad r_i = \frac{d_n^2 N_i}{\Omega}, \quad b = \frac{\sqrt{2} b_0}{\frac{v \ell \rho}{s} d_n^2}, \quad \lambda_i = \frac{\bar{\sigma}_i d_n}{\sqrt{2} b_0}, \quad \tau = \frac{T - T_{pc}}{b T_{pc}}, \quad (13)$$

the excess heat capacity from Eq. (12) becomes

$$c_{exc} \approx \frac{\ell}{T_{pc}} \frac{1}{\sqrt{\pi} b} \sum_{i=1}^n r_i \delta_i^5 e^{-y_i^2} \quad (14)$$

with  $y_i = (\tau \delta_i - \lambda_i) \delta_i$ . The phase change temperature appears in Eq. (14) in the pre-factor as well as in each of the summed terms (via  $\tau$  in the exponent  $y_i$ ). Therefore,  $T_{pc}$  cannot be determined in a straightforward way, using just a single characteristic of the  $c_{exc}$  peak. Instead, several peak's characteristics should be considered simultaneously to determine  $T_{pc}$ . Let us now describe in detail how this can be achieved.

### Procedure for the determination of $T_{pc}$

The domain diameters (represented by  $\delta_i$ ) and the numbers of domains of given diameters (represented by  $r_i$ ) are assumed to be given—from experiment, modeling, or plausible conjecture (see [Domain sizes and their distribution](#) section). On the other hand, the phase change temperature  $T_{pc}$  and latent heat  $\ell$  as well as the two parameters  $b$  and  $\lambda_i$  (associated with the surface effects) are unknown. They must be determined from fitting Eq. (14) to experimental data for  $c_{exc}$ , using at least four characteristics of the  $c_{exc}$  peak: three are needed to obtain  $T_{pc}$ ,  $\ell$ , and  $b$  and one or more to obtain  $\lambda_i$ .

The simplest case—when all  $\lambda_i$  are the same ( $\lambda_i = \text{const} = \lambda_0$ )—was already studied in [13]. Then it was

sufficient to consider only four characteristics that were chosen as the area ( $A$ ), maximum temperature ( $T_{\max}$ ), height ( $H$ ), and an asymmetry factor ( $\alpha$ ) of the  $c_{\text{exc}}$  peak. The factor  $\alpha$  is defined as the part of the peak's area  $A$  that lies below  $T_{\max}$ . Thus, by fitting experimental values of the four characteristics  $A, T_{\max}, H$ , and  $\alpha$ , values of the four quantities  $T_{\text{pc}}, \ell, b$ , and  $\lambda_0$  could be fully determined.

In this study, however, we let the values  $\lambda_i$  be varying, changing with domain diameters. Then the simplest choice is that  $\lambda_i$  are equidistant,  $\lambda_{i+1} - \lambda_i = \text{const} = \Delta\lambda$  with  $\Delta\lambda = (\lambda_n - \lambda_1)/(n - 1)$ . We may write  $\lambda_i = \lambda_n - (n - i)\Delta\lambda$ , and there are two parameters ( $\Delta\lambda$  and  $\lambda_n$ ) that specify all values of  $\lambda_i$ . Values of the five quantities  $T_{\text{pc}}, \ell, b, \Delta\lambda$ , and  $\lambda_n$  must be now determined, so that it will be necessary to fit five characteristics of the  $c_{\text{exc}}$  peak. These will be chosen again as  $A, T_{\max}, H$ , and  $\alpha$ , plus we shall consider another asymmetry factor denoted as  $\beta$ . The latter is introduced as the ratio of two areas of the  $c_{\text{exc}}$  peak: one is the peak's area within the range  $T_{\max} - T_- \leq T \leq T_{\max}$  and the other one is peak's area within the range  $T_{\max} \leq T \leq T_{\max} + T_+$ . The temperatures  $T_+$  and  $T_-$  can be chosen individually for each studied peak.

To carry out the fitting, we need to obtain theoretical expressions for these five characteristics of the  $c_{\text{exc}}$  peak. We get the following results. First, the total area coincides with the specific latent heat,

$$A = \ell. \tag{15}$$

This is a consequence of Eq. (9) and the fact that the jump function  $J$  tends to 1 for large temperatures,  $J(\infty) = 1$ . Second, the temperature  $T_{\max}$  at which  $c_{\text{exc}}$  is maximal is given from the condition  $dc_{\text{exc}}/dT = 0$ . Using Eq. (14) and a parameter  $\kappa$  to relate  $T_{\max}$  to  $T_{\text{pc}}$  as  $T_{\max} = (1 + \kappa b)T_{\text{pc}}$ , the condition may be expressed as

$$\sum_{i=1}^n r_i \delta_i^7 z_i e^{-z_i^2} = 0 \tag{16}$$

with  $z_i = y_i(T_{\max}) = (\kappa\delta_i - \lambda_i)\delta_i = [\kappa\delta_i - \lambda_n + (n - i)\Delta\lambda]\delta_i$ . Next, the height

$$H_{\text{th}} = c_{\text{exc}}(T_{\max}) \approx \frac{A}{bT_{\text{pc}}} \vartheta, \quad \vartheta = \frac{1}{\sqrt{\pi}} \sum_{i=1}^n r_i \delta_i^5 e^{-z_i^2}, \tag{17}$$

as follows immediately from Eq. (14). Finally, using Eqs. (9) and (15), the jump function  $J(T)$  may be used to obtain the asymmetry factors, namely,

$$\alpha_{\text{th}} = J(T_{\max}), \quad \beta_{\text{th}} = \frac{\alpha_{\text{th}} - J(T_-)}{J(T_+) - \alpha_{\text{th}}}. \tag{18}$$

In addition, we may express the jump function as

$$J \approx \frac{1}{2} \sum_{i=1}^n r_i \delta_i^3 \text{erfc}(-y_i) \tag{19}$$

by Eqs. (9) and (14), where  $\text{erfc}$  is the complementary to the Gauss error function.

Using these theoretical expressions, the determination of the phase change temperature  $T_{\text{pc}}$  may be carried out in several steps as follows. Let a  $c_{\text{exc}}$  peak be known from experiment and let  $A, T_{\max}, H$ , and  $\alpha$  and  $\beta$  be the values of its area, maximum temperature, height, and asymmetry factors, respectively.

1. Equation (16) is solved for  $\kappa$ , using a set of values of  $\lambda_n$  and  $\Delta\lambda$ . The dependence  $\kappa(\lambda_n, \Delta\lambda)$  of  $\kappa$  on  $\lambda_n$  and  $\Delta\lambda$  is thus calculated.
2. Using  $\kappa(\lambda_n, \Delta\lambda)$ , the theoretical dependence  $\alpha_{\text{th}}(\lambda_n, \Delta\lambda)$  of the asymmetry factor on  $\lambda_n$  and  $\Delta\lambda$  is calculated from Eqs. (18) and (19).
3. Requiring that  $\alpha_{\text{th}}(\lambda_n, \Delta\lambda) = \alpha$ , a dependence  $\lambda_n(\Delta\lambda)$  of  $\lambda_n$  on  $\Delta\lambda$  is obtained.
4. The dependence  $\vartheta(\lambda_n(\Delta\lambda), \Delta\lambda)$  of  $\vartheta$  on  $\Delta\lambda$  is calculated from Eq. (17).
5. The theoretical dependence  $\beta_{\text{th}}(\lambda_n(\Delta\lambda), \Delta\lambda)$  of the other asymmetry factor on  $\Delta\lambda$  is calculated from Eqs. (18) and (19).
6. Requiring that  $\beta_{\text{th}}(\lambda_n(\Delta\lambda), \Delta\lambda) = \beta$ , the value of  $\Delta\lambda$  is obtained. Knowing  $\Delta\lambda$ , we determine the values of  $\lambda_n, \vartheta$ , and  $\kappa$ , using the results from steps 2–4.
7. Since  $T_{\max} = (1 + \kappa b)T_{\text{pc}}$  and  $bT_{\text{pc}} = A\vartheta/H_{\text{th}}$ , the phase change temperature is  $T_{\text{pc}} = T_{\max} - \kappa bT_{\text{pc}} = T_{\max} - \kappa A\vartheta/H$ , where we required that  $H_{\text{th}}$  be equal to  $H$ .

Note that all five theoretical parameters  $\ell, \lambda_n, \Delta\lambda, T_{\text{pc}}$ , and  $b$  are actually determined during this procedure and not just the phase change temperature (the latter parameter is  $b = bT_{\text{pc}}/T_{\text{pc}} = A\vartheta/HT_{\text{pc}}$ ).

### Domain sizes and their distribution

To apply the above-described procedure, it is necessary to know the values of  $\delta_i$  (the domain diameters) and  $r_i \text{ext}_i$  (essentially, the numbers of domains of given diameters) for a given PCM. These could be obtained from experiment and may be complex. Nevertheless, it is possible to use their simple but realistic approximations due to the term  $r_i \delta_i^5 \propto N_i \delta_i^5$  in Eq. (14). The reason is as follows. Even though the number of domains of a given diameter should decrease with the diameter (i.e.,  $N_i$  drops as  $i$  approaches  $n$ ), the growth of  $\delta_i^5$  with  $i$  is expected to be faster (recall that  $0 < \delta_1 < \delta_2 < \dots < \delta_{n-1} < \delta_n = 1$ ). Altogether  $r_i \delta_i^5$  should be the largest for large domains (i.e., for  $i$  close to  $n$ ) and it

should be practically negligible for small domains. Therefore, while  $\delta_i$  and  $r_i$  may in general depend on  $i$  in a complex way for various PCMs, it is plausible to consider their simple approximations within a narrow range of  $i$  that correspond to predominant contributions to  $c_{exc}$  and extend these approximations to all  $i$ .

To approximate the values of  $\delta_i$ , we use the observation that the differences between the diameters of small domains should be much smaller than between the diameters of large domains; i.e., the differences  $\delta_{i+1} - \delta_i$  should be increasing. A fractal modeling of PCMs with spherical domains suggests a hyperbolic increase [31]. For large domains this can be well approximated by a linear increase,  $\delta_{i+1} - \delta_i = \text{const} \cdot i$ . In an explicit form,

$$\delta_i = \delta_1 + \frac{i(i-1)}{n} \Delta\delta, \quad \Delta\delta = \frac{1-\delta_1}{n-1} > 0. \tag{20}$$

As for the values of  $r_i$ , two approximations will be used here.

In one the numbers of domains of given diameters will be all equal,  $N_i = \text{const}$ , implying  $r_i = \text{const}$  as well. Within this approximation the effect of the domain size distribution  $r_i$  is ignored and the dominant contributions to  $c_{exc}$  (those with  $r_i \delta_i^5$  maximal) are determined by the domain sizes alone: they come from the largest domains; i.e., for  $i = n$  and few  $i$  just below  $n$ .

In the other approximation  $N_i \neq \text{const}$ , so that the effect of  $r_i$  will be taken into account. The number of domains of a given diameter should be decreasing with the diameter, and we shall assume the simplest case of a linear decrease,  $N_i = N_n + (n-i)\Delta N$  with  $\Delta N = (N_1 - N_n)/(n-1) > 0$ . Estimating that  $N_1$  is to  $N_n$  as is the largest domain volume to the smallest one (i.e.,  $N_n/N_1 = \delta_1^3$ ), we get

$$r_i = \frac{q_i}{G}, \quad q_i = \frac{N_i}{N_1} = \delta_1^3 + (n-i)\Delta q, \quad \Delta q = \frac{1-\delta_1^3}{n-1} > 0, \tag{21}$$

where the constant  $G = \Omega/N_1 d_n^3$ . Within this approximation,  $r_i$  linearly decreases with  $i$ , and the predominant contributions (those with  $r_i \delta_i^5$  maximal) are from the domains of diameters of about  $10/11 \approx 0.91$  of the largest domain diameter; i.e., for few  $i$  around  $i = 0.91n$ .

### Determination of $T_{pc}$ for the three materials

We choose the number of different domain sizes to be  $n = 200$  and the smallest domain size to be a tenth of the largest one,  $\delta_1 = 0.1$ . The dependence  $\kappa(\lambda_n, \Delta\lambda)$  of  $\kappa$  on  $\lambda_n$  and  $\Delta\lambda$  is purely theoretical, following from Eq. (16), and thus independent of a specific PCM. It turns out that  $\kappa$  can be very precisely approximated by a linear function of  $\lambda_n$  and  $\Delta\lambda$ . Namely, by  $1.02\lambda_n - 3.30\Delta\lambda$  for the constant  $r_i$  and by  $1.23\lambda_n - 25.37\Delta\lambda$  for the linear  $r_i$ , the corresponding

coefficients of determination  $R^2$  being 0.9996 and 0.9999, respectively.

Knowing  $\kappa(\lambda_n, \Delta\lambda)$ , the dependences of the parameters  $\lambda_n$ ,  $\vartheta$ , and  $\beta_{th}$  on  $\Delta\lambda$  for the three studied materials can be obtained by the above-described procedure. They are plotted in Fig. 3. The temperatures  $T_-$  and  $T_+$  needed to calculate  $\beta_{th}$  were chosen as  $T_- = T_+ = 1\text{K}$  for RT27,  $T_- = 0.9\text{K}$  and  $T_+ = 0.3\text{K}$  for CBC9CB, and  $T_- = T_+ = 0.05\text{K}$  for C23. The equality  $\beta_{th} = \beta$  yields the values of  $\Delta\lambda$  that subsequently yields the values of all other parameters, including the phase change temperature  $T_{pc}$ . The procedure is easy to perceive from the plots in Fig. 3. The results for all three materials are listed in Table 1. In Fig. 4 we show the peaks in the excess heat capacity  $c_{exc}$  of all three materials given by Eq. (14) with the parameters from Table 1. The agreement with experimental data is rather accurate (see Table 2). Moreover, the difference between the peaks obtained for linear and constant  $r_i$  is practically negligible (see Table 2).

In general, it is expected that  $T_{pc}$  should lie within the phase change region; i.e., the difference between  $T_{pc}$  and  $T_{max}$  should be less than about two half-widths of the  $c_{exc}$  peak,  $|T_{pc} - T_{max}| \lesssim 2W_{1/2}$ . Table 1 shows that for CBC9CB this difference is reasonably large, between one and two half-widths of the  $c_{exc}$  peak. Similarly, for C23 the difference is also reasonable, around one half-width of the  $c_{exc}$  peak. For RT27 the difference is less than two half-widths when the linear  $r_i$  is considered, but it is as large as 8.7 of the half-width for a less realistic, constant  $r_i$ . This indicates that it may be important to use proper values of the domain size distribution (proper  $r_i$ ) for those PCMs whose heat capacity peaks are very asymmetric, like RT27.

To understand why  $T_{pc}$  lies above or below  $T_{max}$ , we may recall that the excess heat capacity  $c_{exc}$  is a sum of peaks  $r_i \delta_i^5 \exp(-y_i^2)$  (see Eq. (14)). These peaks have heights  $r_i \delta_i^5$  and their maxima are at temperatures  $T_i = (1 + b\lambda_i/\delta_i)T_{pc}$ . As  $i$  changes from 1 to  $n$ , both the peak's height and maximum temperature change (see Fig. 5). As for the height, it (a) increases with  $i$  from 1 to  $n$  for a constant  $r_i$ , and (b) increases with  $i$  up to about  $0.9n$  and then it decreases for a linear  $r_i$  (see the text below Eqs. (20) and (21)). As for the maximum temperature  $T_i$ , it lies below  $T_{pc}$  when  $\lambda_i < 0$ , while it lies above  $T_{pc}$  when  $\lambda_i > 0$ . Now, the maximum of  $c_{exc}$  at  $T_{max}$  should be close to the position of the tallest peaks. As just argued, the tallest peaks have labels  $i$  that are near  $n$  for a constant  $r_i$  and near  $0.9n$  for a linear  $r_i$ . We thus conclude that if  $\lambda_i < 0$  (if  $\lambda_i > 0$ ) for these labels  $i$ , then the tallest peaks as well as  $T_{max}$  are below  $T_{pc}$  (above  $T_{pc}$ ). For the three studied materials the values of  $\lambda_n$  are given in Table 1 and the values of  $\lambda_{i=0.9n}$  are given in Table 3. For RT27 and C23 the values  $\lambda_i$  are negative both for  $i$  near  $n$  (when  $r_i$  is constant) and near  $0.9n$  (when  $r_i$  is linear), and so their phase change temperatures lie above  $T_{max}$ . On the other hand, for



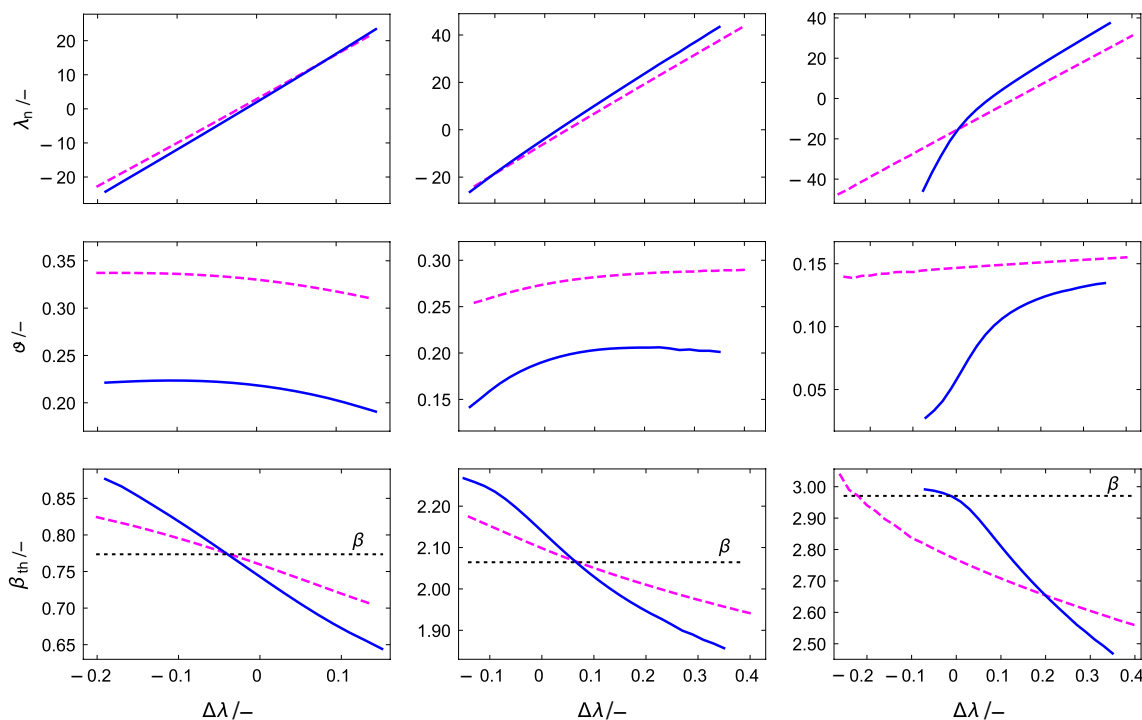


**Fig. 3** The dependences of the parameters  $\lambda_n$ ,  $\vartheta$ , and  $\beta_{th}$  on  $\Delta\lambda$  for the three studied materials. The full lines correspond to the linear  $r_i$  and the dashed ones to the constant  $r_i$

CBC9CB the values  $\lambda_i$  are positive both for  $i$  near  $n$  (when  $r_i$  is constant) and  $i$  near  $0.9n$  (when  $r_i$  is linear), so that its phase change temperature lies below  $T_{max}$ . These qualitative conclusions are confirmed by Table 1 where the calculated values of  $T_{pc}$  are given.

We finally verify the criterion  $(\eta/d_i)^2 \leq 1/K$  with  $K \gg 1$  required in Eq. (11). The criterion specifies the range of possible domain sizes, because it may be rewritten as

$$d_n \geq \left( \sqrt{\frac{K}{\pi}} \frac{4k_B T_{pc}}{v \rho \ell b \delta_1} \right)^{1/3}. \tag{22}$$

Using the values of  $T_{pc}$ ,  $b$ , and  $\ell = A$  from Table 1 and taking  $v = \pi/6$  (spherical domains) and  $K = 10$ , say, the diameter  $d_n$  of the largest domains should be at least a few tens to a few hundreds of nm, which are realistic bounds.

### Conclusions

An improvement of our original technique to describe heat capacity peaks of PCMs was presented. The improvement consists in a more realistic approximation of surface effects in the individual domains of which PCMs are composed. Our main focus was the determination of the phase change temperature  $T_{pc}$  (introduced as the temperature at which the enthalpy would have a jump in the thermodynamic limit).

We pointed out that  $T_{pc}$  cannot be obtained directly from one or two characteristics of a heat capacity peak. Instead, it was necessary to consider five characteristics: peak’s area, maximum position, height, and two asymmetry factors. Determining theoretical expressions for these five quantities and requiring that their values are equal to those from experiment, a procedure to obtain  $T_{pc}$  (plus four other parameters) was presented. The obtained heat capacity peaks very accurately agreed with the experimental ones. Of two considered domain size distributions—a constant  $r_i$  and a linear  $r_i$ —the linear distribution was more appropriate, even for a rather asymmetric heat capacity peak of RT27. Then the obtained values of  $T_{pc}$  lie within the phase change regions of all three considered materials. This indicates that the domain size distribution of a given PCM should be actually used in the determination of its  $T_{pc}$  (which is a topic to be further studied). All these results were calculated under the assumption that kinetic effects were negligible and a PCM was free from effects like thermal hysteresis and supercooling. Good understanding of such plain cases could allow for the analysis of PCMs with a more complicated behavior in the future.

**Acknowledgements** The research in this paper was supported by grants VEGA 1/0682/19 and RVO:11000. The authors would like to thank Prof. Christ Glorieux and Dr. Jan Leys from the Catholic University of Leuven, Belgium, for providing experimental data.

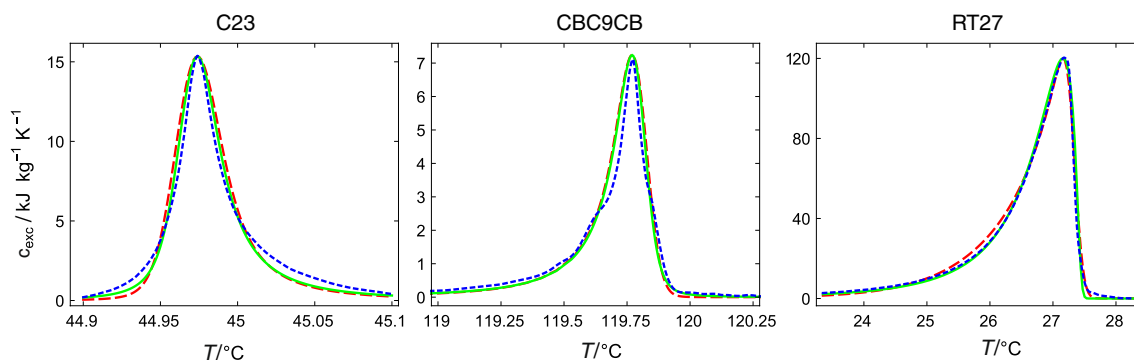


Fig. 4 The excess heat capacity obtained from experiment (dotted lines) and from Eq. (14) for linear  $r_i$  (full lines) and constant  $r_i$  (dashed lines)

Table 1 The values of the experimental and theoretical parameters for the three considered materials

|                                   | Quantity                           | RT27   | CBC9CB | C23    | Unit                             |
|-----------------------------------|------------------------------------|--------|--------|--------|----------------------------------|
| From experiment                   | Area $A$                           | 132.14 | 1.63   | 0.73   | $\text{kJ kg}^{-1}$              |
|                                   | Maximum temp. $T_{\max}$           | 27.16  | 119.77 | 44.97  | $^{\circ}\text{C}$               |
|                                   | Height $H$                         | 120.18 | 7.24   | 15.34  | $\text{kJ kg}^{-1}\text{K}^{-1}$ |
|                                   | Half-width $W_{1/2}$               | 0.78   | 0.12   | 0.03   | $\text{K}, ^{\circ}\text{C}$     |
|                                   | Asymmetry $\alpha$                 | 0.811  | 0.682  | 0.395  | –                                |
|                                   | Asymmetry $\beta$                  | 2.971  | 2.064  | 0.774  | –                                |
| From theory with a constant $r_i$ | $\Delta\lambda$                    | -0.220 | 0.069  | -0.037 | –                                |
|                                   | $\lambda_n$                        | -42.65 | 3.08   | -1.89  | –                                |
|                                   | $\vartheta$                        | 0.140  | 0.280  | 0.333  | –                                |
|                                   | Phase change temp. $T_{\text{pc}}$ | 33.90  | 119.61 | 45.00  | $^{\circ}\text{C}$               |
|                                   | $b \times 10^5$                    | 50.26  | 16.05  | 4.98   | –                                |
| From theory with a linear $r_i$   | $\Delta\lambda$                    | -0.013 | 0.066  | -0.040 | –                                |
|                                   | $\lambda_n$                        | -22.13 | 5.48   | -3.60  | –                                |
|                                   | $\vartheta$                        | 0.049  | 0.200  | 0.222  | –                                |
|                                   | Phase change temp. $T_{\text{pc}}$ | 28.63  | 119.55 | 45.01  | $^{\circ}\text{C}$               |
|                                   | $b \times 10^5$                    | 18.02  | 11.49  | 3.32   | –                                |
| From [13]                         | Phase change temp. $T_{\text{pc}}$ | 30.43  | 120.23 | 44.91  | $^{\circ}\text{C}$               |

Theoretical values of the specific latent heat  $\ell$  are not listed, because they coincide with the values of area  $A$  (see Eq. (15))

Table 2 The coefficients of determination  $R^2$  and ratios of the root mean square error RMSE to peak heights  $H$  for the theoretical vs. experimental excess heat capacities  $c_{\text{exc}}$  of the three materials

|                                  | Quantity   | RT27  | CBC9CB | C23   |
|----------------------------------|------------|-------|--------|-------|
| A constant $r_i$                 | $R^2(-)$   | 0.994 | 0.951  | 0.948 |
|                                  | RMSE/H (%) | 2.1   | 4.0    | 5.9   |
| A linear $r_i$                   | $R^2(-)$   | 0.991 | 0.962  | 0.977 |
|                                  | RMSE/H (%) | 2.6   | 3.5    | 3.9   |
| Between the two choices of $r_i$ | RMSE/H (%) | 2.3   | 0.9    | 2.5   |

Author contributions All authors contributed to the study conception and design. The idea for the article was due to Igor Medved' and Anton

Trník. Analysis was performed by Igor Medved' and Milan Jurči. The first draft of the manuscript was written by Igor Medved' and all authors

Table 3 The theoretical parameters  $\lambda_1$  and  $\lambda_{0.9n} = 0.9\lambda_n + 0.1\lambda_1$  for the three considered materials when the linear  $r_i$  is considered

|                     | Quantity         | RT27   | CBC9CB | C23   | Unit |
|---------------------|------------------|--------|--------|-------|------|
| From theory         | $\lambda_1$      | -19.58 | -7.64  | 4.32  | –    |
| With a linear $r_i$ | $\lambda_{0.9n}$ | -21.88 | 4.17   | -2.80 | –    |

commented on previous versions of the manuscript. All authors read and approved the final manuscript

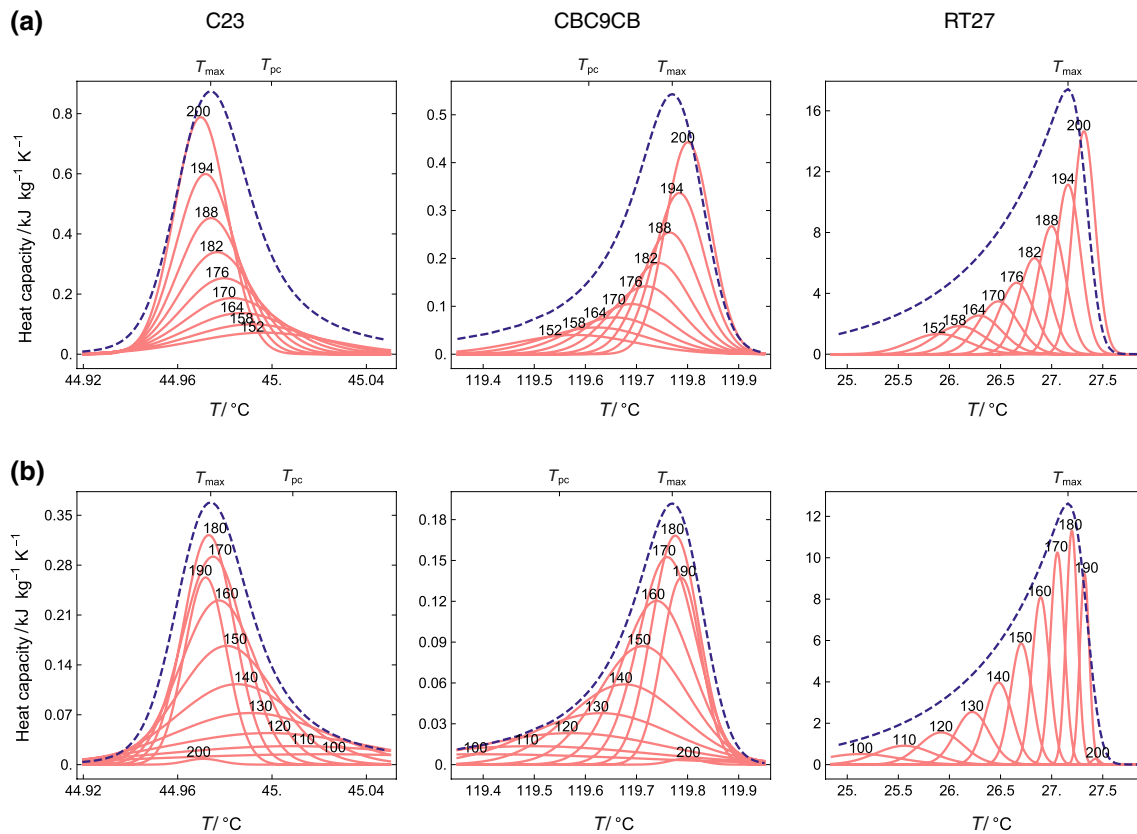


**Fig. 5** Selected peaks (full lines) in the sum from Eq. (14) for the excess heat capacity  $c_{\text{exc}}$  for the case of **a** a constant  $r_i$  and **b** a linear  $r_i$ . The labels  $i$  of the selected peaks are indicated. The dashed lines

represent  $c_{\text{exc}}$  multiplied by a suitably small constant to make it fit the plot. The determined phase change temperature  $T_{\text{pc}}$  for RT27 lies beyond the depicted temperature interval and it is therefore not shown

## References

- Zhou D, Zhao CY, Tian Y. Review on thermal energy storage with phase change materials (PCMs) in building applications. *Appl Energy*. 2012;92:593–605.
- Cabeza LF, Castell A, Barreneche C, de Gracia A, Fernández AI. Materials used as PCM in thermal energy storage in buildings: a review. *Renew Sust Energy Rev*. 2011;15:1675–95.
- Oró E, de Gracia A, Castell A, Farid MM, Cabeza LF. Review on phase change materials (PCMs) for cold thermal energy storage applications. *Appl Energy*. 2012;99:513–33.
- Zhao Y, Zhang XL, Xu XF. Application and research progress of cold storage technology in cold chain transportation and distribution. *J Therm Anal Calorim*. 2020;139:1419–34.
- Akeiber H, Nejat P, Majid MZA, Wahid MA, Jomehzadeh F, Zeynali Famileh I, Calautit JK, Hughes BR, Zaki SA. A review on phase change material (PCM) for sustainable passive cooling in building envelopes. *Renew Sust Energy Rev*. 2016;60:1470–97.
- Kenisarin M, Mahkamov K. Solar energy storage using phase change materials. *Renew Sust Energy Rev*. 2007;11:1913–65.
- Xu B, Li P, Chan C. Application of phase change materials for thermal energy storage in concentrated solar thermal power plants: a review to recent developments. *Appl Energy*. 2015;160:286–307.
- Omara AAM, Abuelnuor AAA, Mohammed HA, Khiadani M. Phase change materials (PCMs) for improving solar still productivity: a review. *J Therm Anal Calorim*. 2020;139:1585–617.
- Rao Z, Wang S. A review of power battery thermal energy management. *Renew Sust Energy Rev*. 2011;15:4554–71.
- Ling Z, Zhang Z, Shi G, Fang X, Wang L, Gao X, Fang Y, Xu T, Wang S, Liu X. Review on thermal management systems using phase change materials for electronic components, Li-ion batteries and photovoltaic modules. *Renew Sust Energy Rev*. 2014;31:427–38.
- Sarier N, Onder E. Organic phase change materials and their textile applications: an overview. *Thermochim Acta*. 2012;540:7–60.
- Mehling H, Cabeza LF. Heat and cold storage with PCM. Berlin: Springer; 2008.
- Medved' I, Trník A, Vozár L. Modeling of heat capacity peaks and enthalpy jumps of phase-change materials used for thermal energy storage. *Int J Heat Mass Transf*. 2017;107:123–32.
- Leys J, Duponchel B, Longuemart S, Glorieux C, Thoen J. A new calorimetric technique for phase change materials and its application to alkane-based PCMS. *Mater Renew Sustain Energy*. 2016;5:4.
- Tripathi CSP, Losada-Pérez P, Glorieux C, Kohlmeier A, Tamba MG, Mehl GH, Leys J. Nematic-nematic phase transition in the liquid crystal dimer CBC9CB and its mixtures with 5CB: a high-resolution adiabatic scanning calorimetric study. *Phys Rev E*. 2011;84:041707.
- Losada-Pérez P, Tripathi CSP, Leys J, Cordoyiannis G, Glorieux C, Thoen J. Measurements of heat capacity and enthalpy of phase change materials by adiabatic scanning calorimetry. *Int J Thermophys*. 2011;32:913–24.
- Thoen J, Cordoyiannis G, Glorieux C. Adiabatic scanning calorimetry investigation of the melting and order-disorder

- phase transitions in the linear alkanes heptadecane and nonadecane and some of their binary mixtures. *J Chem Thermodyn.* 2021;163:106596.
18. Borgs C, Kotecký R. Finite-size effects at asymmetric first-order phase transitions. *Phys Rev Lett.* 1992;68:1734–7.
  19. Borgs C, Kotecký R. Surface-induced finite-size effects for first-order phase transitions. *J Stat Phys.* 1995;79:43–115.
  20. Boldyreva EV, Drebuschak VA, Drebuschak TN, Paukov IE, Kovalevskaya YA, Shutova ES. Polymorphism of glycine: thermodynamic aspects. Part i - Relative stability of the polymorphs. *J Therm Anal Calorim.* 2003;73:409–18.
  21. Boldyreva EV, Drebuschak VA, Drebuschak TN, Paukov IE, Kovalevskaya YA, Shutova ES. Polymorphism of glycine: thermodynamic aspects. Part ii - Polymorphic transitions. *J Therm Anal Calorim.* 2003;73:419–28.
  22. Minkov VS, Drebuschak VA, Ogienko AG, Boldyreva EV. Decreasing particle size helps to preserve metastable polymorphs. A case study of dl-cysteine. *CrystEngComm.* 2011;13:4417–26.
  23. Sahoo SC, Panda MK, Nath NK, Naumov P. Biomimetic crystalline actuators: structure-kinematic aspects of the self-actuation and motility of thermosalient crystals. *J Am Chem Soc.* 2013;135:12241–51.
  24. Seki T, Mashimo T, Ito H. Anisotropic strain release in a thermosalient crystal: correlation between the microscopic orientation of molecular rearrangements and the macroscopic mechanical motion. *Chem Sci.* 2019;10:4185–91.
  25. Smets MMH, Kalkman E, Krieger A, Tinnemans P, Meekes H, Vlieg E, Cuppen HM. On the mechanism of solid-state phase transitions in molecular crystals—the role of cooperative motion in (quasi)racemic linear amino acids. *IUCrJ.* 2020;7:331–41.
  26. Herrero E, Buller LJ, Abruña HD. Underpotential deposition at single crystal surfaces of Au, Pt, Ag and other materials. *Chem Rev.* 2001;101:1897–930.
  27. Huckaby DA, Blum L. A model for sequential 1st-order phase transitions occurring in the underpotential deposition of metals. *J Electroanal Chem.* 1991;315:255–61.
  28. Blum L, Huckaby DA. Phase transitions at liquid-solid interfaces: Padé approximant to adsorption isotherms and voltammograms. *J Chem Phys.* 1991;94:6887–94.
  29. Huckaby DA, Medved' I. Shapes of voltammogram spikes explained as resulting from the effects of finite electrode crystal size. *J Chem Phys.* 2002;117:2914–22.
  30. Medved' I, Huckaby DA. Voltammogram spikes interpreted as envelopes of spikes resulting from electrode crystals of various sizes: application to the UPD of Cu on Au(111). *J Chem Phys.* 2003;118:11147–59.
  31. Jurči M, Medved' I. Fractal modeling of polycrystalline PCMs. *AIP Conf Proc.* 2020;2275:020021.

**Publisher's Note** Springer Nature remains neutral with regard to jurisdictional claims in published maps and institutional affiliations.